

# Embedded Delaunay tori and their Willmore energy

Christian Scharrer \*

June 1, 2022

## Abstract

A family of embedded rotationally symmetric tori in the Euclidean 3-space consisting of two opposite signed constant mean curvature surfaces that converge as varifolds to a double round sphere is constructed. Using complete elliptic integrals, it is shown that their Willmore energy lies strictly below  $8\pi$ . Combining such a strict inequality with previous works by KELLER–MONDINO–RIVIÈRE and MONDINO–SCHARRER allows to conclude that for every isoperimetric ratio there exists a smoothly embedded torus minimising the Willmore functional under isoperimetric constraint, thus completing the solution of the isoperimetric-constrained Willmore problem for tori. Similarly, we deduce the existence of smoothly embedded tori minimising the Helfrich functional with small spontaneous curvature. Moreover, it is shown that the tori degenerate in the moduli space which gives an application also to the conformally-constrained Willmore problem. Finally, because of their symmetry, the Delaunay tori can be used to construct spheres of high isoperimetric ratio, leading to an alternative proof of the known result for the genus zero case.

## 1 Introduction

Given an immersed surface  $f : \Sigma \rightarrow \mathbb{R}^3$ , the Willmore functional  $\mathcal{W}$  at  $f$  is defined by

$$\mathcal{W}(f) = \int_{\Sigma} H^2 \, d\mu,$$

where the mean curvature  $H$  is given by the arithmetic mean of the two principal curvatures, and  $\mu$  is the Radon measure on  $\Sigma$  corresponding to the pull back metric of the Euclidean metric in  $\mathbb{R}^3$  along  $f$ . The isoperimetric ratio is defined by

$$\text{iso}(f) = \begin{cases} \frac{\text{area}(f)^2}{\text{vol}(f)^{\frac{2}{3}}} & \text{if } \text{vol}(f) > 0, \\ \infty & \text{if } \text{vol}(f) \leq 0, \end{cases} \quad (1.1)$$

where

$$\text{area}(f) = \int_{\Sigma} 1 \, d\mu, \quad \text{vol}(f) = \frac{1}{3} \int_{\Sigma} n \cdot f \, d\mu \quad (1.2)$$

---

\*Max Planck Institute for Mathematics, Vivatsgasse 7, 53111 Bonn, Germany. Email: [Scharrer@mpim-bonn.mpg.de](mailto:Scharrer@mpim-bonn.mpg.de).

are the area and algebraic volume, and  $n : \Sigma \rightarrow \mathbb{S}^2$  is the Gauß map.

The aim of this paper is to construct a family of embedded  $C^{1,1}$ -regular tori  $\mathbb{T}_{D,c}$  in  $\mathbb{R}^3$  corresponding to  $1 < c < \gamma_0$  for some constant  $\gamma_0 > 1$ . The tori are rotationally symmetric and converge for  $c \rightarrow 1$  as varifolds to a round sphere of multiplicity 2 and radius 2. They are constructed out of two kinds of constant mean curvature surfaces that are well known in literature as *Delaunay surfaces* (see [Del41]): The inner part of the tori has constant, strictly positive mean curvature; the outer part has constant, strictly negative mean curvature. These two pieces of Delaunay surfaces have matching normal vectors along the curve of intersection, leading to  $C^{1,1}$ -regularity of the patched surface. For a picture of the profile curve, see Figure 5. The tori will be called *Delaunay tori*. Their main property is stated in the following theorem which will be proven in Section 6, using complete elliptic integrals.

**1.1 Theorem.** *There exists  $\gamma_0 > 1$  such that the family of embedded Delaunay tori  $\mathbb{T}_{D,c}$  corresponding to  $1 < c < \gamma_0$  satisfies*

$$\mathcal{W}(\mathbb{T}_{D,c}) < 8\pi \quad \text{whenever } 1 < c < \gamma_0$$

and

$$\lim_{c \rightarrow 1+} \text{iso}(\mathbb{T}_{D,c}) = \infty.$$

In Section 7, it will be shown that the family of Delaunay tori  $\mathbb{T}_{D,c}$  can be used to construct a family of embedded spheres  $\mathbb{S}_{D,c}$  in  $\mathbb{R}^3$  (for a picture of the profile curve, see Figure 9) with the following property.

**1.2 Theorem.** *Let  $\gamma_0 > 1$  be such that the Delaunay tori  $\mathbb{T}_{D,c}$  exist for all  $1 < c < \gamma_0$ . Then, the family of spheres  $\mathbb{S}_{D,c}$  satisfies*

$$\mathcal{W}(\mathbb{S}_{D,c}) = 4\pi + \frac{\mathcal{W}(\mathbb{T}_{D,c})}{2} \quad \text{for all } 1 < c < \gamma_0$$

as well as

$$\lim_{c \rightarrow 1+} \text{iso}(\mathbb{S}_{D,c}) = \infty.$$

There are different notions of isoperimetric ratio in literature all of which are scaling invariant. The definition in this paper (1.1) is the same as in [MS21] but differs from [Sch12] and [KMR14]. Nevertheless, it is easy to see that Theorem 1.2 together with Theorem 1.1 provides an alternative proof of the known result for spheres [Sch12, Lemma 1].

Denote with  $\mathcal{S}_1$  the space of smoothly immersed tori in  $\mathbb{R}^3$ . As a consequence of the Euclidean isoperimetric inequality, the isoperimetric ratio is minimised exactly by any parametrisation of a round sphere. Indeed, the round sphere is the only closed stable constant mean curvature surface [BdC84]. On the other hand, each smoothly embedded closed surface in  $\mathbb{R}^3$  can be smoothly transformed arbitrarily close to a round sphere. This can be done using a one parameter family of Möbius transformations whose centres

of inversion approach a point on the surface (see [Sch21, Proposition 1] and [YC22, Theorem 3.1]). It follows that

$$\text{iso}[\mathcal{S}_1] = (\sqrt[3]{36\pi}, \infty]$$

where  $\text{iso}(\mathbb{S}^2) = \sqrt[3]{36\pi}$ . The following main application will be proven in Section 6; the proof will follow by combining Theorem 1.1 with previous works of KELLER–MONDINO–RIVIÈRE [KMR14] and MONDINO–SCHARRER [MS21].

**1.3 Corollary.** *Let  $\sqrt[3]{36\pi} < \sigma < \infty$ . Then, there holds*

$$\beta_1(\sigma) := \inf\{\mathcal{W}(f) \mid f \in \mathcal{S}_1, \text{iso}(f) = \sigma\} < 8\pi \quad (1.3)$$

*and the infimum in (1.3) is attained by a smoothly embedded minimiser  $f_0 \in \mathcal{S}_1$ .*

This completes the solution for the existence (and regularity) problem of isoperimetric constrained minimisers for the Willmore functional in the genus one case. The genus zero case was solved by SCHYGULLA [Sch12]. Notice that Corollary 1.3 is stated for all  $\sigma \in \text{iso}[\mathcal{S}_1]$  while Theorem 1.1 only holds for high isoperimetric ratios  $\sigma$ . In fact, the crucial part of the strict inequality 1.3 is exactly that it holds true for high isoperimetric ratios. Indeed, the function  $\beta_1$  is non-decreasing in  $\sigma$ , see [Sch21, Theorem 3.15] and [MS21, Corollary 1.6].

Given an immersed surface  $f : \Sigma \rightarrow \mathbb{R}^3$  and  $c_0 \in \mathbb{R}$ , the *Helfrich functional*  $\mathcal{H}_{c_0}$  at  $f$  is defined by

$$\mathcal{H}_{c_0}(f) = \int_{\Sigma} (H - c_0)^2 d\mu.$$

In order to study the shape of lipid bilayer cell membranes, HELFRICH [Hel73] proposed the minimisation of  $\mathcal{H}_{c_0}$  in the class of closed surfaces with given fixed area and given fixed volume. The constant  $c_0$  is referred to as *spontaneous curvature*. Existence of minimisers in the class of (possibly branched and bubbled) spheres was proven by MONDINO–SCHARRER [MS20]. Existence and regularity for minimisers with higher genus remains an open problem. Partial results were obtained by CHOKSI–VENERONI [CV13], EICHMANN [Eic20], and BRAZDA–LUSSARDI–STEFANELLI [BLS20]. Denote with  $\mathcal{S}_0$  the space of smoothly immersed spheres in  $\mathbb{R}^3$  and for all  $\sigma > \sqrt[3]{36\pi}$  let

$$\beta_0(\sigma) = \inf\{\mathcal{W}(f) \mid f \in \mathcal{S}_0, \text{iso}(f) = \sigma\}.$$

Suppose  $A_0, V_0 > 0$  satisfy the isoperimetric inequality:  $A_0^3 > 36\pi V_0^2$ . Then, by Corollary 1.3 and [MS21, Corollary 1.5], the following constant is strictly positive:

$$\varepsilon(A_0, V_0) := \frac{\sqrt{\min\{8\pi, 2\pi^2 + \beta_0(A_0/V_0^{2/3}) - 4\pi\}} - \sqrt{\beta_1(A_0/V_0^{2/3})}}{2\sqrt{A_0}} > 0. \quad (1.4)$$

As another application of Theorem 1.1, the following result on the existence of Helfrich tori will be proven in Section 8.

**1.4 Corollary.** *Suppose  $A_0, V_0 > 0$  satisfy the isoperimetric inequality:  $A_0^3 > 36\pi V_0^2$  and let  $\varepsilon = \varepsilon(A_0, V_0)$  be defined as in Equation (1.4). Then, for each  $c_0 \in (-\varepsilon, \varepsilon)$ , there exists a smoothly embedded torus  $f_0 \in \mathcal{S}_1$  with*

$$\text{area}(f_0) = A_0, \quad \text{vol}(f_0) = V_0$$

and

$$\mathcal{H}_{c_0}(f_0) = \inf\{\mathcal{H}_{c_0}(f) \mid f \in \mathcal{S}_1, \text{area}(f) = A_0, \text{vol}(f) = V_0\}.$$

A further application of Theorem 1.1 can be found in the context of conformally constrained minimisation. We define the moduli space  $\mathcal{M}$  for tori as a subset of the complex plane by

$$\mathcal{M} := \{x + iy \in \mathbb{C} \mid -1/2 \leq x \leq 1/2, y > 0, x^2 + y^2 \geq 1\}.$$

Any torus is conformally equivalent to a quotient  $T_\omega^2 := \mathbb{C}/(\mathbb{Z} + \omega\mathbb{Z})$  endowed with the Euclidean metric for some  $\omega \in \mathcal{M}$ , cf. [IT92]. Following NDIAYE–SCHÄTZLE [NS15], we let

$$\mathcal{M}_{3,1}(\omega) := \inf\{\mathcal{W}(f) \mid f : T_\omega^2 \rightarrow \mathbb{R}^3 \text{ is conformal}\}. \quad (1.5)$$

The following corollary can be found in NDIAYE–SCHÄTZLE [NS15, Proposition D.1]. In Section 6, we will show how the Delaunay tori and Theorem 1.1 provide an alternative proof to the one in [NS15].

**1.5 Corollary.** *There exists a constant  $y_0 > 1$  such that*

$$\mathcal{M}_{3,1}(iy) < 8\pi \quad \text{for } y \geq y_0. \quad (1.6)$$

Recently, DALL’ACQUA–MÜLLER–SCHÄTZLE–SPENER [DMSS20] proved that the Willmore flow of rotationally symmetric tori with initial energy at most  $8\pi$  stays rotationally symmetric, exists for all times, and converges to the Clifford torus. The conformal class depends continuously on the time (see [DMSS20, Proposition 4.2]) while the Willmore energy is non-increasing in time. Consequently, since the conformal class of the Clifford torus is represented by the complex number  $\omega = i$ , the function  $\mathcal{M}_{3,1}(iy)$  is non-increasing in  $y \geq 1$ . In particular, the strict inequality in (1.6) becomes valid for all  $y \geq 1$ . Hence, by KUWERT–SCHÄTZLE [KS13], the infimum  $\mathcal{M}_{3,1}(iy)$  for  $y \geq 1$  in (1.5) is attained by a smooth minimiser. For an existence result on the conformally constrained minimisation that does not rely on an  $8\pi$ -bound, see RIVIÈRE [Riv14, Riv15]. Explicit minimisers can be found in [NS14, NS15, HN21].

In many classical problems related to the minimisation of the Willmore functional, strict  $8\pi$ -bounds such as in Equation (1.3) or Corollary 1.5 play a crucial role. One of the reasons is that by the *Li–Yau inequality* [LY82], any immersed surface with Willmore energy strictly below  $8\pi$  is actually embedded. Exemplary for the importance of  $8\pi$ -bounds is the Willmore flow. KUWERT–SCHÄTZLE [KS04] showed that the Willmore flow of spheres exists for all time and converges to a round sphere provided the initial surface has Willmore energy less than  $8\pi$ . Later, BLATT [Bla09] showed that this energy threshold is

actually sharp. Recently, DALL’ACQUA–MÜLLER–SCHÄTZLE–SPENER [DMSS20] showed that the same energy threshold is also sharp for the long time existence of the Willmore flow of rotationally symmetric tori. Equally important,  $8\pi$ -bounds are needed in the direct method of the calculus of variations for the minimisation of the Willmore functional. This relates to the classical Willmore problem, the conformally constrained Willmore problem, and the isoperimetric constrained Willmore problem. In what follows, we illustrate the importance of  $8\pi$ -bounds for the Willmore functional in literature and point out potential directions for future research.

In the early 60s, WILLMORE [Wil65] showed that the energy now bearing his name is bounded from below by  $4\pi$  on the class of closed surfaces, with equality only for the round sphere. This inequality is sometimes referred to as *Willmore’s inequality*. More than two decades later, in an interesting work that connects Willmore surfaces with minimal surfaces, KUSNER [Kus89] estimated the area of the celebrated *Lawson surfaces* [Law70]. KUSNER’s work [Kus89] led to the  $8\pi$ -bound for the unconstrained minimal Willmore energy amongst surfaces of arbitrary genus. This was one of the key steps in proving existence and regularity of minimisers for the classical minimisation problem proposed by WILLMORE [Wil65]. Roughly speaking, the  $8\pi$  bound prevents macroscopic bubbling in the direct method of calculus of variations, as by Willmore’s inequality, each of the bubbles would cost at least  $4\pi$  energy. Indeed, already SIMON [Sim93] used the  $8\pi$ -bound to obtain compactness (up to suitable Möbius renormalisations) in the so called *ambient approach*. Later, the  $8\pi$ -bound was also used in the *parametric approach* to obtain compactness in the moduli space of higher genus surfaces by independent papers of KUWERT–LI [KL12] (building on top of previous work of MÜLLER–ŠVERÁK [MŠ95]) and RIVIÈRE [Riv13] (building on top of HÉLEIN’s moving frames technique [Hél02]).

Existence of smoothly embedded isoperimetric constrained Willmore spheres was proven by SCHYGULLA [Sch12]. Inspired by the computations of CASTRO-VILLARREAL–GUVEN [CVG07], SCHYGULLA [Sch12] applied a family of sphere inversions to a complete catenoid resulting in a family of closed surfaces with arbitrarily high isoperimetric ratios having one point of multiplicity two and Willmore energy exactly  $8\pi$ . Subsequently, they applied the Willmore flow for a short time around the point of multiplicity two, to obtain a family of surfaces with Willmore energy strictly below  $8\pi$  and arbitrarily high isoperimetric ratios. This proved the strict  $8\pi$ -bound for isoperimetric constrained spheres. Moreover, SCHYGULLA [Sch12] showed that, as varifolds, isoperimetric constrained Willmore spheres (as well as the inverted catenoids) converge to a round sphere of multiplicity 2 as the isoperimetric ratio tends to infinity. Notice that the same holds true for the family of Delaunay tori constructed in this paper. His blow up result was analysed in more detail by KUWERT–LI [KL18]. They showed that any sequence of isoperimetric constrained Willmore spheres whose isoperimetric ratios diverge to infinity, indeed converges (up to subsequences, scaling, and translating) to two concentric round spheres of almost the same radii connected by a catenoidal neck. These kind of surfaces (i.e. two concentric round spheres of nearly the same radii connected by one or more catenoidal necks) were also constructed by means of cutting and paste techniques for different purposes in the works of KÜHNEL–PINKALL [KP86], MÜLLER–RÖGER [MR14], NDIAYE–SCHÄTZLE [NS15], and

WOJTOWYTSCH [Woj17]. One of the advantages of this technique is that it produces not only tori but surfaces of any topological type.

It is very natural to expect that, provided higher genus isoperimetric constrained minimisers exist, the blow up result of KUWERT–LI [KL18] can be generalised to the higher genus cases. To be more precise, we expect that any sequence of genus  $g$  isoperimetric constrained Willmore surfaces whose isoperimetric ratios diverge to infinity, converges (up to subsequences, scaling, and translating) to two concentric round spheres of nearly the same radii connected by  $g + 1$  catenoidal necks. It is an interesting question whether or not the catenoidal necks in the limit have to be distributed over the double sphere in a certain way. In view of the solution presented in this paper, it is of course very tempting to conjecture that the catenoidal necks have to satisfy a balancing condition analogous to the one for constant mean curvature surfaces, see for instance KAPOULEAS [Kap91, Kap95], or KOREVAAR–KUSNER–SOLOMON [KKS89]. That would mean that for tori, the two catenoidal necks necessarily end up being antipodal.

**Acknowledgements.** The author was supported by the EPSRC as part of the MASDOC DTC at the University of Warwick, Grant No. EP/HO23364/1. Moreover, the author would like to thank ANDREA MONDINO, FILIP RINDLER, and PETER TOPPING for hints and discussions on the subject. The author would also like to thank the referee for their careful reading of the original manuscript.

## 2 Elliptic integrals

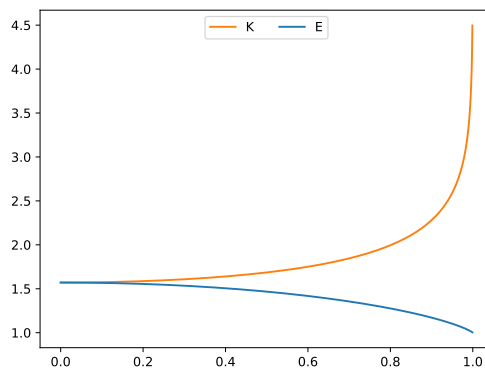


Figure 1: Complete elliptic integrals of the first and the second kind.

Elliptic integrals are functions defined as the value of common types of integrals that cannot be expressed in terms of elementary functions. They arise when computing geometric quantities such as the arc length of an ellipse or a hyperbola. In particular, they naturally occur in the context of constant mean curvature (Delaunay) surfaces of revolution. This is because the rotating curves of Delaunay surfaces are given by the roulette generated by ellipses and hyperbolas. In fact, all the quantities that are

needed to construct the family of embedded Delaunay tori (see Section 6) as well as their Willmore energy can be expressed in terms of *complete elliptic integrals*. Given a so-called *elliptic modulus*  $k$ , that is a real number  $0 < k < 1$ , the *complete elliptic integral of the first kind*  $K$  and the *complete elliptic integral of the second kind*  $E$  are defined by

$$K(k) = \int_0^{\pi/2} \frac{d\theta}{\sqrt{1 - k^2 \sin^2(\theta)}}, \quad E(k) = \int_0^{\pi/2} \sqrt{1 - k^2 \sin^2(\theta)} d\theta.$$

All the formulas for elliptic integrals used in this paper can be found in the book of BYRD–FRIEDMAN [BF71]. The derivatives are given by

$$\frac{dK(k)}{dk} = \frac{E(k)}{k(1 - k^2)} - \frac{K(k)}{k}, \quad \frac{dE(k)}{dk} = \frac{E(k) - K(k)}{k}.$$

The *Gauß transformation* works as follows. Define the *complementary modulus*  $k'$  and the transformed modulus  $k_1$  by

$$k' = \sqrt{1 - k^2}, \quad k_1 = \frac{1 - k'}{1 + k'}.$$

Then, there holds (see [BF71, 164.02])

$$K(k) = (1 + k_1)K(k_1), \quad E(k) = (1 + k')E(k_1) - k'(1 + k_1)K(k_1). \quad (2.1)$$

Moreover,  $K$  grows like  $\log(1/k')$ , namely

$$\lim_{k \rightarrow 1^-} \left( K(k) - \log(4/\sqrt{1 - k^2}) \right) = 0 \quad (2.2)$$

and  $E$  is bounded:

$$1 \leq E \leq \pi/2. \quad (2.3)$$

### 3 Surfaces of revolution

A surface of revolution in  $\mathbb{R}^3$  is given by a parametrisation  $X$  of the type

$$X(t, \theta) = (f(t) \cos(\theta), f(t) \sin(\theta), g(t))$$

with parameters  $t$  lying in an open interval and  $0 \leq \theta \leq 2\pi$ , where  $f, g$  are real valued functions. The rotating curve  $\gamma := (f, g)$  is referred to as *meridian* or *profile curve*. The underlying geometry is described by the coefficients of the first fundamental form

$$E^I = X_t \cdot X_t = \dot{f}^2 + \dot{g}^2 = |\dot{\gamma}|^2, \quad F^I = X_t \cdot X_\theta = 0, \quad G^I = X_\theta \cdot X_\theta = f^2$$

and the second fundamental form

$$L^{II} = X_{tt} \cdot n = \frac{\dot{f}\ddot{g} - \ddot{f}\dot{g}}{|\dot{\gamma}|}, \quad M^{II} = X_{t\theta} \cdot n = 0, \quad N^{II} = X_{\theta\theta} \cdot n = \frac{f\dot{g}}{|\dot{\gamma}|}$$

where the Gauß map  $n$  is given by

$$n = \frac{X_t \times X_\theta}{|X_t \times X_\theta|}.$$

The mean curvature  $H$  is defined as the arithmetic mean of the principal curvatures  $\kappa_1, \kappa_2$ , that is

$$2H = \kappa_1 + \kappa_2 = \frac{L^{II}}{E^I} + \frac{N^{II}}{G^I} = \frac{\dot{f}\ddot{g} - \ddot{f}\dot{g}}{|\dot{\gamma}|^3} + \frac{\dot{g}}{f|\dot{\gamma}|}.$$

In this paper, we will focus on surfaces of revolution with constant mean curvature

$$H = \frac{1}{2a} \tag{3.1}$$

for some given  $0 \neq a \in \mathbb{R}$ . These surfaces arise as critical points of the volume constrained area functional. Outside of a discrete set, one has  $\dot{g} \neq 0$  and thus  $\gamma(\varphi(t)) = (\rho(t), t)$  for some parameter transform  $\varphi$  and some real valued function  $\rho$ . Hence, outside of a discrete set, Equation (3.1) can be turned into a second order ODE. Its solutions were first described by DELAUNAY [Del41] and are now named after him. More precisely, solutions for  $a > 0$  are called *unduloids* and will be discussed in Section 4; solutions for  $a < 0$  are called *nodoids* and will be discussed in Section 5.

## 4 Unduloids

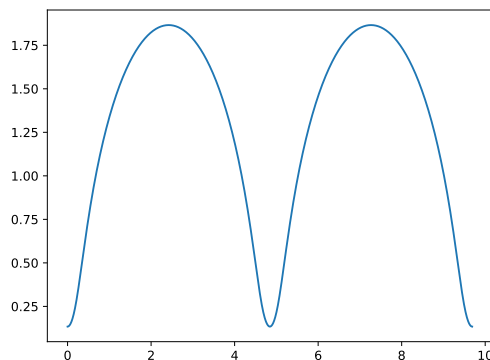


Figure 2: Profile curve of an unduloid with  $a = 1$ ,  $b = 0.5$  where the  $f$ -axis is vertical and the  $g$ -axis is horizontal.

Unduloids are surfaces of revolution with constant, strictly positive mean curvature. Their rotating curve  $(f, g)$  is given by the roulette of an ellipse with generating point being one of the foci. To be more precise, let  $a > b > 0$  and define  $c = \sqrt{a^2 - b^2}$ . Then, the equation

$$\frac{x^2}{a^2} + \frac{y^2}{b^2} = 1$$



describes a standard ellipse centred at the origin with width  $2a$ , height  $2b$ , and foci  $\pm c$  on the  $x$ -axis. Rolling the ellipse without slipping along a line, each of the two focus points will describe a curve, *the roulette*. This curve is *periodic* in the following sense, where one period corresponds to one round of the ellipse: There exist a parametrisation  $(f, g)$  of the roulette as well as  $\lambda > 0$  and  $L \in \mathbb{R}$  referred to as *period length* and *extrinsic period length* such that

$$\begin{aligned} f(t + k\lambda) &= f(t) \\ g(t + k\lambda) &= g(t) + kL \end{aligned} \tag{4.1}$$

for all  $t \in \mathbb{R}$  and all  $k \in \mathbb{Z}$ . Indeed, the extrinsic length  $L$  is given by the circumference of the ellipse, see (4.7). Figure 2 shows two periods of the roulette using the following parametrisation found by BENDITO–BOWICK–MEDINA [BBM14] with period length  $\lambda = 2\pi$ :

$$f(t) = b \frac{a - c \cos(t)}{\sqrt{a^2 - c^2 \cos^2(t)}} \tag{4.2}$$

$$g(t) = \int_0^t \sqrt{a^2 - c^2 \cos^2(x)} \, dx - c \sin(t) \frac{a - c \cos(t)}{\sqrt{a^2 - c^2 \cos^2(t)}} \tag{4.3}$$

for  $0 \leq t \leq 2\pi$  with coefficients of the first fundamental form

$$E^I = \frac{a^2 b^2}{(a + c \cos(t))^2}, \quad G^I = b^2 \frac{a - c \cos(t)}{a + c \cos(t)},$$

speed

$$|(f, g)'(t)| = \frac{ab}{a + c \cos(t)}, \tag{4.4}$$

and mean curvature

$$H = \frac{1}{2a}. \tag{4.5}$$

The extrema are given by

$$\min \text{image } f = f(0) = a - c, \quad \max \text{image } f = f(\pi) = a + c. \tag{4.6}$$

## 4.1 Extrinsic period length

We compute the extrinsic length  $L$  of one period. Using the parametrisation (4.3), we see

$$\begin{aligned} L &= |g(2\pi) - g(0)| = a \int_0^{2\pi} \sqrt{1 - \frac{c^2}{a^2} \cos^2(x)} \, dx = 4a \int_0^{\pi/2} \sqrt{\left(1 - \frac{c^2}{a^2}\right) + \frac{c^2}{a^2} \sin^2(x)} \, dx \\ &= 4a \sqrt{1 - \frac{c^2}{a^2}} \int_0^{\pi/2} \sqrt{1 + n^2 \sin^2(x)} \, dx \end{aligned}$$

for  $n = c/b$ . Letting  $k^2 = n^2/(1 + n^2)$ , (282.03) and (315.02) in [BF71] imply

$$\int_0^{\pi/2} \sqrt{1 + n^2 \sin^2(x)} \, dx = \frac{1}{k'} E(k),$$

where we used the special values  $\text{sn}(0) = 0$  and  $\text{cd}(K) = 0$  taken from (122.01), (122.02), and (120.02) in [BF71]. Thus, since

$$k = \frac{c}{a}, \quad k' = \sqrt{1 - \frac{c^2}{a^2}},$$

it follows that

$$L = 4aE(k); \quad k = \frac{c}{a}. \quad (4.7)$$

## 4.2 Area computation

Next, a formula for the area will be determined. Using the Weierstraß substitution, the area  $\mathcal{A}$  of the rotational symmetric surface corresponding to one period can be computed by

$$\begin{aligned} \int_0^{2\pi} \int_0^{2\pi} \sqrt{EG} \, d\theta \, dt &= 2\pi ab^2 \int_0^{2\pi} \sqrt{\frac{a - c \cos(t)}{(a + c \cos(t))^3}} \, dt = 4\pi ab^2 \int_0^\pi \sqrt{\frac{a + c \cos(t)}{(a - c \cos(t))^3}} \, dt \\ &= 4\pi ab^2 \int_0^\infty \sqrt{\frac{a + c \frac{1-x^2}{1+x^2}}{(a - c \frac{1-x^2}{1+x^2})^3}} \frac{2dx}{1+x^2} = 8\pi ab^2 \int_0^\infty \sqrt{\frac{a(1+x^2) + c(1-x^2)}{(a(1+x^2) - c(1-x^2))^3}} \, dx \\ &= 8\pi ab^2 \int_0^\infty \sqrt{\frac{(a+c) + (a-c)x^2}{((a-c) + (a+c)x^2)^3}} \, dx = 8\pi ab^2 \sqrt{\frac{a-c}{(a+c)^3}} \int_0^\infty \sqrt{\frac{\tilde{a}^2 + t^2}{(\tilde{b}^2 + t^2)^3}} \, dt \end{aligned}$$

for  $\tilde{a}^2 = (a+c)/(a-c)$  and  $\tilde{b}^2 = (a-c)/(a+c)$ . The last integral can be transformed into a complete elliptic integral of the second kind using [BF71, 221.01] with  $k^2 = 1 - \tilde{b}^2/\tilde{a}^2$  and  $g = 1/\tilde{a}$ :

$$\int_0^\infty \sqrt{\frac{\tilde{a}^2 + t^2}{(\tilde{b}^2 + t^2)^3}} \, dt = \frac{g}{k'^2} E(k).$$

One can show that

$$k^2 = \frac{4ac}{(a+c)^2}, \quad k' = \frac{a-c}{a+c}, \quad \frac{g}{k'^2} = \frac{(a+c)^{3/2}}{(a-c)^{3/2}}$$

and thus

$$\mathcal{A} = 8\pi a(a+c)E(k); \quad k = \frac{2\sqrt{ac}}{a+c}. \quad (4.8)$$

Notice that this coincides with the area formula for unduloids computed for a different parametrisation in [HMO07] and [MO03].

## 4.3 Volume computation

One can show that for  $g$  as defined in (4.3) there holds

$$g'(t) = ab^2 \frac{a - c \cos(t)}{(a^2 - c^2 \cos^2(t))^{\frac{3}{2}}}.$$

Hence, using the Weierstraß substitution, the volume  $\mathcal{V}$  of the rotational symmetric surface corresponding to one period can be computed as

$$\begin{aligned}
\mathcal{V} &= \pi \int_0^{2\pi} f^2 g' dt = 2\pi ab^4 \int_0^\pi \sqrt{\frac{a + c \cos(t)}{(a - c \cos(t))^5}} dt = 4\pi ab^4 \int_0^\infty \sqrt{\frac{a + c \frac{1-x^2}{1+x^2}}{(a - c \frac{1-x^2}{1+x^2})^5}} \frac{dx}{1+x^2} \\
&= 4\pi ab^4 \int_0^\infty \sqrt{\frac{a + c + (a - c)x^2}{(a - c + (a + c)x^2)^5}} (1 + x^2) dx \\
&= 4\pi ab^4 \int_0^{\frac{\pi}{2}} \sqrt{\frac{a + c + (a - c)\frac{a-c}{a+c} \tan^2(s)}{(a - c + (a + c)\frac{a-c}{a+c} \tan^2(s))^5}} \left(1 + \frac{a - c}{a + c} \tan^2(s)\right) \sqrt{\frac{a - c}{a + c}} \frac{ds}{\cos^2(s)} \\
&= 4\pi a \int_0^{\frac{\pi}{2}} \sqrt{(a + c)^2 \cos^2(s) + (a - c)^2 \sin^2(s)} \left((a + c) \cos^2(s) + (a - c) \sin^2(s)\right) ds.
\end{aligned}$$

The last line can be expressed in terms of complete elliptic integrals. For the purpose of this paper it is enough to notice that

$$\mathcal{V} \xrightarrow{b \downarrow 0} 16\pi a^3 \int_0^{\frac{\pi}{2}} \cos^3(s) ds = \frac{4\pi}{3} (2a)^3. \quad (4.9)$$

## 5 Nodoids

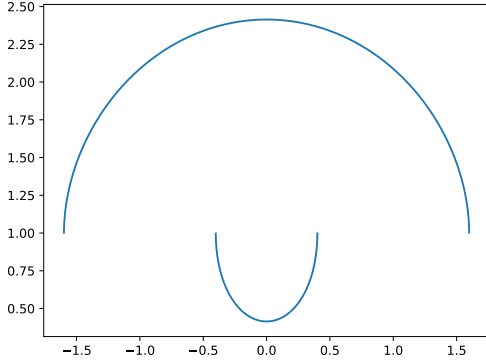


Figure 3: Separate roulettes ( $f_\pm, g_\pm$ ) (bottom/top) for  $a = b = 1$ .

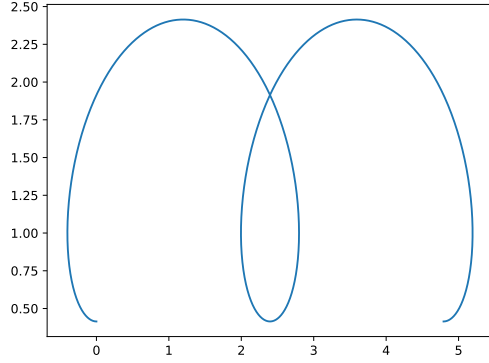


Figure 4: Both roulettes patched together for 2 periods and  $a = b = 1$ .

Nodoids are surfaces of revolution with constant, strictly negative mean curvature. Their rotating curve  $(f, g)$  is given by the roulette of a hyperbola with generating points given by the foci. To be more precise, let  $a, b > 0$  and define  $c = \sqrt{a^2 + b^2}$ . Then, the equation

$$\frac{x^2}{a^2} - \frac{y^2}{b^2} = 1$$

describes a hyperbola in canonical form with distance  $a$  to the centre and foci  $\pm c$  on the  $x$ -axis. Rolling the right branch of the hyperbola without slipping along a line, each of the

two focus points will describe a curve, *the roulette*. BENDITO–BOWICK–MEDINA [BBM14] found parametrisations  $(f_{\pm}, g_{\pm})$  of the roulettes, where  $(f_{+}, g_{+})$  corresponds to the focus  $(c, 0)$  and  $(f_{-}, g_{-})$  is the reflected roulette corresponding to the focus  $(-c, 0)$ :

$$f_{\pm}(t) = b \frac{c \cosh(t) \mp a}{\sqrt{c^2 \cosh^2(t) - a^2}} \quad (5.1)$$

$$g_{\pm}(t) = \int_0^t \sqrt{c^2 \cosh^2(x) - a^2} dx - c \sinh(t) \frac{c \cosh(t) \mp a}{\sqrt{c^2 \cosh^2(t) - a^2}} \quad (5.2)$$

with parameter  $t$  running through all of  $\mathbb{R}$ , coefficients of the first fundamental form

$$E_{\pm} = \frac{a^2 b^2}{(c \cosh(t) \pm a)^2}, \quad G_{\pm} = b^2 \frac{c \cosh(t) \mp a}{c \cosh(t) \pm a},$$

speed

$$|(f_{\pm}, g_{\pm})'(t)| = \frac{ab}{c \cosh(t) \pm a}, \quad (5.3)$$

and mean curvature

$$H_{\pm} = -\frac{1}{2a}. \quad (5.4)$$

One has

$$\begin{aligned} \max \text{ image } f_{+} &= \lim_{t \rightarrow \pm\infty} f_{+}(t) = b, & \min \text{ image } f_{+} &= f_{+}(0) = c - a \\ \min \text{ image } f_{-} &= \lim_{t \rightarrow \pm\infty} f_{-}(t) = b, & \max \text{ image } f_{-} &= f_{-}(0) = c + a \end{aligned} \quad (5.5)$$

and thus, after translation along the axis of rotation, the two roulettes corresponding to the foci  $(\pm c, 0)$  can be glued together into one curve. After suitable reparametrisation, this curve can be extended to a *periodic* curve, i.e. a curve that satisfies (4.1), see Figure 4. Analysing the ODE (5.4), one can show that the curve obtained by glueing is  $C^2$ -regular, see Equation (3.3), Proposition 3, and Proposition 5 in [MP01]. Indeed, in Section 5.1, we will give a smooth parametrisation of the glued curve.

## 5.1 Extrinsic period length

In order to determine the extrinsic length  $L$  of one period, we perform the parameter transformation  $t = \operatorname{arsinh}(u)$  and  $u = \frac{b}{c} \tan(s)$  for  $-\frac{\pi}{2} < s < \frac{\pi}{2}$ . We have

$$\begin{aligned} f_{\pm}(t) &= b \frac{c\sqrt{1+u^2} \mp a}{\sqrt{c^2(1+u^2) - a^2}} = \frac{c\sqrt{1+u^2} \mp a}{\sqrt{1 + \frac{c^2}{b^2}u^2}} = \frac{c\sqrt{1 + \frac{b^2}{c^2}\tan^2(s)} \mp a}{\sqrt{1 + \tan^2(s)}} \\ &= \sqrt{c^2 \cos^2(s) + b^2 \sin^2(s)} \mp a \cos(s) \end{aligned} \quad (5.6)$$

and

$$\begin{aligned}
\int_0^t \sqrt{c^2 \cosh^2(x) - a^2} \, dx &= \int_0^u \sqrt{\frac{c^2(1+x^2) - a^2}{1+x^2}} \, dx = \frac{b}{c} \int_0^{\tan(s)} \sqrt{\frac{c^2 \frac{b^2}{c^2} x^2 + b^2}{1 + \frac{b^2}{c^2} x^2}} \, dx \\
&= b^2 \int_0^s \sqrt{\frac{1 + \tan^2(x)}{c^2 + b^2 \tan^2(x)}} \tan'(x) \, dx = b^2 \int_0^s \frac{\tan'(x) \, dx}{\sqrt{c^2 \cos^2(x) + b^2 \sin^2(x)}} \\
&= -b^2 \int_0^s \frac{a^2 \sin(x) \cos(x)}{(c^2 - a^2 \sin^2(x))^{\frac{3}{2}}} \tan(x) \, dx + b^2 \frac{\tan(s)}{\sqrt{b^2 + a^2 \cos^2(s)}}.
\end{aligned}$$

Moreover, there holds  $c \sinh(t) = b \tan(s)$  and

$$\begin{aligned}
\tan(s) &\left[ \frac{b^2}{\sqrt{b^2 + a^2 \cos^2(s)}} - \sqrt{b^2 + a^2 \cos^2(s)} \pm a \cos(s) \right] \\
&= -a^2 \frac{\sin(s) \cos(s)}{\sqrt{b^2 + a^2 \cos^2(s)}} \pm a \sin(s).
\end{aligned}$$

It follows

$$g_{\pm}(s) = -a^2 b^2 \int_0^s \frac{\sin^2(x) \, dx}{(c^2 - a^2 \sin^2(x))^{\frac{3}{2}}} - a^2 \frac{\sin(s) \cos(s)}{\sqrt{b^2 + a^2 \cos^2(s)}} \pm a \sin(s). \quad (5.7)$$

Define  $k^2 = a^2/c^2$  and

$$L = \frac{4k^2 b^2}{c} \int_0^{\pi/2} \frac{\sin^2(x) \, dx}{(1 - k^2 \sin^2(x))^{\frac{3}{2}}}. \quad (5.8)$$

Extending the definition of the functions  $f_{\pm}$  and  $g_{\pm}$  in (5.6) and (5.7) for all  $s \in \mathbb{R}$ , one readily verifies

$$f_{\pm}(s + \pi) = f_{\mp}(s), \quad g_{\pm}(s + \pi) = -\frac{L}{2} + g_{\mp}(s) \quad (5.9)$$

and thus

$$f_{\pm}(s + 2\pi) = f_{\pm}(s), \quad g_{\pm}(s + 2\pi) = -L + g_{\pm}(s).$$

Hence, we see that both curves  $\mathbb{R} \rightarrow \mathbb{R}^2$  with  $s \mapsto (f_+(s), g_+(s))$  and  $s \mapsto (f_-(s), g_-(s))$  parametrise the whole periodic curve resulting from the patched roulettes in Figure 4 with period length  $\lambda = 2\pi$  and extrinsic period length  $-L$  given in (5.8), cf. (4.1). These curves are smooth. Using (281.05), (318.02) from [BF71] as well as the special values  $\text{sn}(0) = \text{cd}(K) = 0$ , we find

$$L = 4c \left[ E(k) - k'^2 K(k) \right]; \quad k = \frac{a}{c}. \quad (5.10)$$

## 5.2 Area computation

Next, the area  $\mathcal{A}$  of the rotational symmetric surface corresponding to one period will be computed. Using the parameter transformations  $t = \operatorname{artanh}(x)$  and  $x = \sin(t)$ , one infers

$$\begin{aligned} \int_{-\infty}^{\infty} \sqrt{E_+ G_+} dt &= ab^2 \int_{-\infty}^{\infty} \sqrt{\frac{c \cosh(t) - a}{(c \cosh(t) + a)^3}} dt = 2ab^2 \int_0^1 \sqrt{\frac{c \frac{1}{\sqrt{1-x^2}} - a}{(c \frac{1}{\sqrt{1-x^2}} + a)^3}} \frac{dx}{1-x^2} \\ &= 2ab^2 \int_0^1 \sqrt{\frac{c - a\sqrt{1-x^2}}{(c + a\sqrt{1-x^2})^3}} \frac{dx}{\sqrt{1-x^2}} = 2ab^2 \int_0^{\pi/2} \sqrt{\frac{c - a \cos(t)}{(c + a \cos(t))^3}} dt \\ &= 2ab^2 \int_{\pi/2}^{\pi} \sqrt{\frac{c + a \cos(t)}{(c - a \cos(t))^3}} dt \end{aligned}$$

and similarly,

$$\int_{-\infty}^{\infty} \sqrt{E_- G_-} dt = 2ab^2 \int_0^{\pi/2} \sqrt{\frac{c + a \cos(t)}{(c - a \cos(t))^3}} dt.$$

Consequently,

$$\mathcal{A} = \int_0^{2\pi} \int_{-\infty}^{\infty} \sqrt{E_+ G_+} + \sqrt{E_- G_-} dt d\theta = 4\pi ab^2 \int_0^{\pi} \sqrt{\frac{c + a \cos(t)}{(c - a \cos(t))^3}} dt.$$

In Section 4 it was shown that

$$\int_0^{\pi} \sqrt{\frac{c + a \cos(t)}{(c - a \cos(t))^3}} dt = \frac{2E(k)}{c - a}; \quad k = \frac{2\sqrt{ac}}{a + c}.$$

Thus, it follows that

$$\mathcal{A} = 8\pi a(a + c)E(k); \quad k = \frac{2\sqrt{ac}}{a + c}. \quad (5.11)$$

## 5.3 Volume computation

Using the parametrisation in (5.6) and (5.7), we find

$$\begin{aligned} f_{\pm}(s)^2 &= 2a^2 \cos^2(s) + b^2 \mp 2a \cos(s) \sqrt{a^2 \cos^2(s) + b^2}, \\ g'_{\pm}(s) &= -\frac{a^2 \cos^2(s)}{\sqrt{a^2 \cos^2(s) + b^2}} \pm a \cos(s). \end{aligned}$$

We compute

$$\begin{aligned} f_{\pm}^2 g'_{\pm} &= \frac{1}{\sqrt{a^2 \cos^2 + b^2}} \left[ -(2a^2 \cos^2 + b^2) a^2 \cos^2 - 2a^2 \cos^2 (a^2 \cos^2 + b^2) \right] \\ &\quad \pm (2a^2 \cos^2 + b^2) a \cos \pm 2a^3 \cos^3. \end{aligned}$$

Now, in view of (5.9), the (orientation dependent) volume  $\mathcal{V}$  of the rotational symmetric surface corresponding to one period can be computed as

$$\begin{aligned}\mathcal{V} &= \pi \int_{-\frac{\pi}{2}}^{\frac{\pi}{2}} f_-^2 g'_- \, ds + \pi \int_{-\frac{\pi}{2}}^{\frac{\pi}{2}} f_+^2 g'_+ \, ds = \pi \int_{-\pi}^{\pi} f_-^2 g'_- \, ds \\ &= -4\pi a^2 \int_0^{\frac{\pi}{2}} \frac{4a^2 \cos^4(s) + 3b^2 \cos^2(s)}{\sqrt{a^2 \cos^2(s) + b^2}} \, ds.\end{aligned}$$

This integral can be expressed in terms of complete elliptic integrals. For the purpose of this paper it is enough to notice that

$$\mathcal{V} \xrightarrow{b \downarrow 0} -\frac{4\pi}{3}(2a)^3. \quad (5.12)$$

## 6 Embedded Delaunay tori

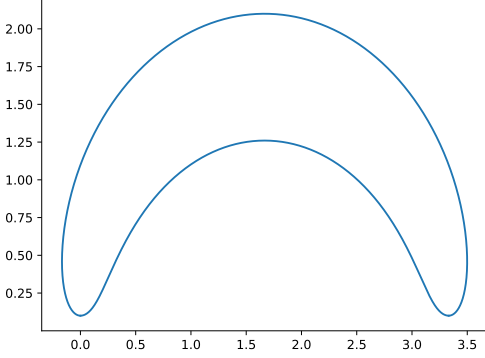


Figure 5: Profile curve Delaunay torus with  $c = 1.1$  and the bottom line being the axis of rotation.

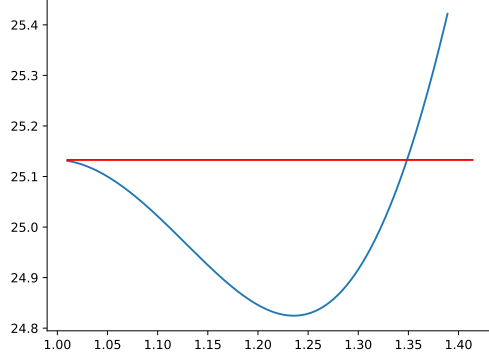


Figure 6: Energy curve for the family of Delaunay tori and  $8\pi$  bound.

In this Section, we will construct the family of embedded Delaunay tori  $\mathbb{T}_{D,c}$  with  $1 < c < \gamma_0$  for some constant  $\gamma_0$  and we will prove Theorem 1.1. Moreover, at the end of this section, we will give a proof of Corollaries 1.3 and 1.5.

Each Delaunay torus is a rotationally symmetric surface whose profile curve (see Figure 5) consists of one period of an unduloid roulette (see Figure 2) and one period of a nodoid roulette (see Figure 4). The construction works as follows. Start with a one parameter family of patched nodoids (see Section 5) running for one period and starting at the point where  $f_+$  attains its minimum according to (5.5), where  $a = 1$  and  $c > 1$  is the free parameter, thus  $b$  is given by  $b = \sqrt{c^2 - 1}$  and the minimum according to (5.5) is  $c - 1$ . Next, depending on the parameter  $c$ , find  $a > y > 0$  such that the unduloid corresponding to the ellipse with foci  $(\pm y, 0)$ , width  $2a$ , and height  $2b$  for  $b = \sqrt{a^2 - y^2}$  (see Section 4) running for one period and starting at the point where  $f$  attains its minimum  $a - y$  according (4.6), fits right into the given nodoid. That means the two end

points where the patched nodoids reach their minimum need to match the two end points where the unduloid reaches its minimum. Notice that, in this way, the profile curve is  $C^{1,1}$ -regular. Indeed, choosing graphical representations around the glueing points (such representations exist since by (4.3),  $g'(0) = g'(2\pi) \neq 0$  and by (5.2),  $g'_-(0) \neq 0$ ), it is clear that the glued curve is  $C^1$ -regular and, since both unduloids and nodoids induce constant mean curvature surfaces, their second derivative is naturally bounded near the gluing point leading to  $C^{1,1}$ -regularity, cf. [MP01, Equation (3.3)]. The coordinates of the two patching points can be determined using Equations (4.6), (4.7) for the unduloid and (5.5), (5.10) for the nodoid. Thus,  $a, y$  are given as the solution of the system of equations

$$\begin{cases} 4aE\left(\frac{y}{a}\right) = 4c \left[ E\left(\frac{1}{c}\right) - \left(1 - \frac{1}{c^2}\right)K\left(\frac{1}{c}\right) \right] \\ a - y = c - 1. \end{cases} \quad (6.1)$$

Abbreviating

$$\varepsilon := c - 1, \quad \Lambda := c \left[ E\left(\frac{1}{c}\right) - \varepsilon \frac{c+1}{c^2} K\left(\frac{1}{c}\right) \right],$$

the system of equations reads as

$$\begin{cases} (y + \varepsilon)E\left(\frac{y}{y + \varepsilon}\right) = \Lambda \\ a = y + \varepsilon. \end{cases}$$

Define the  $C^1$ -function

$$F : (1, \infty) \times (0, \infty) \rightarrow \mathbb{R}, \quad F(c, y) = (y + \varepsilon(c))E\left(\frac{y}{y + \varepsilon(c)}\right) - \Lambda(c).$$

There holds

$$\varepsilon \log \frac{4}{\sqrt{1 - 1/c^2}} = \varepsilon \log \frac{4c}{\sqrt{\varepsilon}\sqrt{c+1}} \leq \frac{4c}{\sqrt{c+1}}\sqrt{\varepsilon} \xrightarrow{c \downarrow 1} 0.$$

Hence, by (2.2) and since  $E(1) = 1$ , we have

$$\lim_{c \rightarrow 1+} \Lambda(c) = 1. \quad (6.3)$$

Moreover,

$$\begin{aligned} \partial_c \Lambda &= [E(\tfrac{1}{c}) - (1 - \tfrac{1}{c^2})K(\tfrac{1}{c})] + c[E(\tfrac{1}{c}) - K(\tfrac{1}{c})]c^{-\frac{1}{c^2}} \\ &\quad + c \left[ \tfrac{-2}{c^3}K(\tfrac{1}{c}) - (1 - \tfrac{1}{c^2})[E(\tfrac{1}{c})/(1 - \tfrac{1}{c^2}) - K(\tfrac{1}{c})]c(\tfrac{-1}{c^2}) \right] = E(\tfrac{1}{c}) - K(\tfrac{1}{c}) \end{aligned}$$

and, for  $k = y/(y + \varepsilon)$

$$\partial_c(F + \Lambda) = E(k) + (y + \varepsilon)[E(k) - K(k)]\frac{y + \varepsilon}{y} \frac{-y}{(y + \varepsilon)^2} = K(k)$$

which implies

$$\partial_c F = K\left(\frac{y}{y + \varepsilon}\right) + K\left(\frac{1}{c}\right) - E\left(\frac{1}{c}\right).$$



Writing  $k = y/(y + \varepsilon)$ , there holds

$$\partial_y F = E(k) + (y + \varepsilon)[E(k) - K(k)] \frac{y + \varepsilon}{y} \frac{\varepsilon}{(y + \varepsilon)^2} = \left(1 + \frac{\varepsilon}{y}\right) E(k) - \frac{\varepsilon}{y} K(k).$$

Moreover, for fixed  $y > 0$ ,

$$\varepsilon \log \frac{4}{\sqrt{1 - y^2/(y + \varepsilon)^2}} = \varepsilon \log \frac{4(y + \varepsilon)}{\sqrt{2\varepsilon y + \varepsilon^2}} \leq \frac{4(y + \varepsilon)}{\sqrt{2y + \varepsilon}} \sqrt{\varepsilon} \xrightarrow{c \downarrow 1} 0 \quad (6.4)$$

and thus, by (2.2),

$$\lim_{c \rightarrow 1+} \partial_y F(c, y) = 1. \quad (6.5)$$

In view of (6.3), we can choose  $1 < \gamma_0 < 1 + (2\pi)^{-1}$  such that  $\Lambda(c) > 1/2$  for all  $1 < c < \gamma_0$ . For such  $c$  it follows that  $\varepsilon(c) \leq (2\pi)^{-1}$  and by (2.3),

$$(y + \varepsilon(c))E\left(\frac{y}{y + \varepsilon(c)}\right) \leq \frac{1}{2}, \quad F(c, y) < 0$$

for all  $y \leq (2\pi)^{-1}$ . On the other hand, using (2.3), we have  $\Lambda(c) \leq \gamma_0 \pi/2 < 3$  and thus  $F(c, y) > 0$  for all  $y \geq 3$ . Therefore, by the intermediate value theorem, we see that for all  $1 < c < \gamma_0$  there exists

$$\frac{1}{2\pi} \leq y(c) \leq 3 \quad (6.6)$$

such that  $F(c, y(c)) = 0$ . Moreover, since  $y(c) \geq (2\pi)^{-1}$ , we can use (6.5) to see that for  $c$  close to 1,  $\partial_y F(c, y(c)) \neq 0$ . Therefore, we can apply the implicit function theorem to obtain  $\gamma_0 > 1$  such that  $y(c)$  is a smooth function in  $c$  for  $1 < c < \gamma_0$  and

$$y' = \frac{E(\frac{1}{c}) - K(\frac{1}{c}) - K(\frac{y}{y + \varepsilon})}{(y + \varepsilon)E(\frac{y}{y + \varepsilon}) - \varepsilon K(\frac{y}{y + \varepsilon})} y. \quad (6.7)$$

Using (4.5), (4.8) for the unduloid and (5.4), (5.11) for the nodoid (with  $c = y$ ,  $a = y + \varepsilon$ ), one obtains the Willmore energy of the Delaunay tori  $\mathbb{T}_{D,c}$ :

$$\mathcal{W}(\mathbb{T}_{D,c}) = \mathcal{W}_{\text{nod}} + \mathcal{W}_{\text{und}} \quad (6.8)$$

where

$$\mathcal{W}_{\text{nod}} = 2\pi(1 + c)E\left(\frac{2\sqrt{c}}{1 + c}\right), \quad \mathcal{W}_{\text{und}} = 2\pi\left(1 + \frac{y}{y + \varepsilon}\right)E\left(\frac{2\sqrt{y(y + \varepsilon)}}{2y + \varepsilon}\right).$$

Using the uniform bound on  $y$  in (6.6), we infer by (6.4), (2.2), and  $E(1) = 1$  that

$$\lim_{c \rightarrow 1+} \frac{y}{y + \varepsilon} = 1, \quad \lim_{c \rightarrow 1+} y = 1, \quad \lim_{c \rightarrow 1+} \varepsilon K\left(\frac{y}{y + \varepsilon}\right) = 0, \quad \lim_{c \rightarrow 1+} \mathcal{W}(\mathbb{T}_{D,c}) = 8\pi.$$

Next, we show that  $\partial_c \mathcal{W}(\mathbb{T}_{D,c}) < 0$  for  $c$  close to 1 which then implies  $\mathcal{W}(\mathbb{T}_{D,c}) < 8\pi$  for  $c$  close to 1. First, we compute  $\partial_c \mathcal{W}_{\text{nod}}$ . For this purpose, let  $k = 2\sqrt{c}/(1 + c)$ . Then,

$$\partial_c k = \frac{1}{(1 + c)\sqrt{c}} - \frac{2\sqrt{c}}{(1 + c)^2} = \frac{1 - c}{(1 + c)^2 \sqrt{c}}$$

and

$$\begin{aligned}\partial_c \mathcal{W}_{\text{nod}} &= 2\pi E(k) + 2\pi(1+c)[E(k) - K(k)] \frac{1+c}{2\sqrt{c}} \frac{1-c}{(1+c)^2\sqrt{c}} \\ &= \pi \left( \left(1 + \frac{1}{c}\right) E(k) + \left(1 - \frac{1}{c}\right) K(k) \right).\end{aligned}$$

By the Gauß transformation (2.1) there hold

$$k' = \sqrt{1 - \frac{4c}{(1+c)^2}} = \frac{c-1}{c+1}, \quad k_1 = \frac{1-k'}{1+k'} = \frac{1}{c},$$

and

$$\frac{\partial_c \mathcal{W}_{\text{nod}}}{\pi} = \left(1 + \frac{1}{c}\right) \left[ \left(1 + \frac{c-1}{c+1}\right) E\left(\frac{1}{c}\right) - \frac{c-1}{c+1} \left(1 + \frac{1}{c}\right) K\left(\frac{1}{c}\right) \right] + \left(1 - \frac{1}{c}\right) \left(1 + \frac{1}{c}\right) K\left(\frac{1}{c}\right) = 2E\left(\frac{1}{c}\right).$$

Hence,

$$\partial_c \mathcal{W}_{\text{nod}} = 2\pi E\left(\frac{1}{c}\right). \quad (6.9)$$

In order to compute  $\partial_y \mathcal{W}_{\text{und}}$ , let  $k = 2\sqrt{y(y+\varepsilon)}/(2y+\varepsilon)$ . Then, there hold

$$\partial_y k = \frac{2y+\varepsilon}{(2y+\varepsilon)\sqrt{y(y+\varepsilon)}} - \frac{4\sqrt{y(y+\varepsilon)}}{(2y+\varepsilon)^2} = \frac{\varepsilon^2}{(2y+\varepsilon)^2\sqrt{y(y+\varepsilon)}}, \quad \partial_y \frac{y}{y+\varepsilon} = \frac{\varepsilon}{(y+\varepsilon)^2}$$

and

$$\begin{aligned}\partial_y \mathcal{W}_{\text{und}} &= 2\pi \frac{\varepsilon}{(y+\varepsilon)^2} E(k) + 2\pi \frac{2y+\varepsilon}{y+\varepsilon} [E(k) - K(k)] \frac{2y+\varepsilon}{2\sqrt{y(y+\varepsilon)}} \frac{\varepsilon^2}{\sqrt{y(y+\varepsilon)}(2y+\varepsilon)^2} \\ &= \frac{\pi\varepsilon}{(y+\varepsilon)^2} (2E(k) + \frac{\varepsilon}{y} [E(k) - K(k)]) = \frac{\pi\varepsilon}{y(y+\varepsilon)^2} ((2y+\varepsilon)E(k) - \varepsilon K(k)).\end{aligned}$$

By the Gauß transformation (2.1) there hold

$$k' = \sqrt{1 - \frac{4y(y+\varepsilon)}{(2y+\varepsilon)^2}} = \frac{\varepsilon}{2y+\varepsilon}, \quad k_1 = \frac{1-k'}{1+k'} = \frac{y}{y+\varepsilon}$$

and

$$\begin{aligned}(2y+\varepsilon)E(k) - \varepsilon K(k) &= (2y+\varepsilon) \left[ \left(1 + \frac{\varepsilon}{2y+\varepsilon}\right) E\left(\frac{y}{y+\varepsilon}\right) - \frac{\varepsilon}{2y+\varepsilon} \left(1 + \frac{y}{y+\varepsilon}\right) K\left(\frac{y}{y+\varepsilon}\right) \right] \\ &\quad - \varepsilon \left(1 + \frac{y}{y+\varepsilon}\right) K\left(\frac{y}{y+\varepsilon}\right) = 2((y+\varepsilon)E\left(\frac{y}{y+\varepsilon}\right) - \varepsilon \left(1 + \frac{y}{y+\varepsilon}\right) K\left(\frac{y}{y+\varepsilon}\right)).\end{aligned} \quad (6.10)$$

Therefore,

$$\partial_y \mathcal{W}_{\text{und}} = \frac{2\pi\varepsilon}{y(y+\varepsilon)^2} \left[ (y+\varepsilon)E\left(\frac{y}{y+\varepsilon}\right) - \varepsilon \left(1 + \frac{y}{y+\varepsilon}\right) K\left(\frac{y}{y+\varepsilon}\right) \right]. \quad (6.11)$$

Abbreviate  $z = y'/y$ , and  $k = y/(y+\varepsilon)$ . Then, (6.11) and (6.7) imply

$$\begin{aligned}\partial_y \mathcal{W}_{\text{und}} \cdot y' &= \frac{2\pi\varepsilon}{y(y+\varepsilon)^2} \left[ (y+\varepsilon)E(k) - \varepsilon \left(1 + \frac{y}{y+\varepsilon}\right) K(k) \right] \cdot \frac{E(\frac{1}{c}) - K(\frac{1}{c}) - K(k)}{(y+\varepsilon)E(k) - \varepsilon K(k)} y \\ &= \frac{2\pi\varepsilon}{(y+\varepsilon)^2} \left[ E\left(\frac{1}{c}\right) - K\left(\frac{1}{c}\right) - K\left(\frac{y}{y+\varepsilon}\right) \right] - \frac{2\pi\varepsilon}{(y+\varepsilon)^2} \frac{\varepsilon y}{y+\varepsilon} z K\left(\frac{y}{y+\varepsilon}\right).\end{aligned} \quad (6.12)$$

Finally we compute  $\partial_\varepsilon \mathcal{W}_{\text{und}}$ . For this purpose let  $k = 2\sqrt{y(y+\varepsilon)}/(2y+\varepsilon)$ . Then, there hold

$$\partial_\varepsilon k = \frac{y}{(2y+\varepsilon)\sqrt{y(y+\varepsilon)}} - \frac{2\sqrt{y(y+\varepsilon)}}{(2y+\varepsilon)^2} = \frac{-y\varepsilon}{(2y+\varepsilon)^2\sqrt{y(y+\varepsilon)}}$$

and

$$\begin{aligned}\partial_\varepsilon \mathcal{W}_{\text{und}} &= 2\pi \frac{-y}{(y+\varepsilon)^2} E(k) + 2\pi \frac{2y+\varepsilon}{y+\varepsilon} [E(k) - K(k)] \frac{2y+\varepsilon}{2\sqrt{y(y+\varepsilon)}} \frac{-y\varepsilon}{(2y+\varepsilon)^2\sqrt{y(y+\varepsilon)}} \\ &= -\frac{\pi}{(y+\varepsilon)^2} ((2y+\varepsilon)E(\frac{y}{y+\varepsilon}) - \varepsilon K(\frac{y}{y+\varepsilon})).\end{aligned}$$

Thus, by (6.10),

$$\partial_\varepsilon \mathcal{W}_{\text{und}} = -\frac{2\pi}{(y+\varepsilon)^2} \left[ (y+\varepsilon)E\left(\frac{y}{y+\varepsilon}\right) - \varepsilon \left(1 + \frac{y}{y+\varepsilon}\right) K\left(\frac{y}{y+\varepsilon}\right) \right].$$

Recall that, by the choice of  $y$ , there holds

$$(y+\varepsilon)E\left(\frac{y}{y+\varepsilon}\right) = c \left[ E\left(\frac{1}{c}\right) - \left(1 - \frac{1}{c^2}\right) K\left(\frac{1}{c}\right) \right].$$

Therefore,

$$\partial_\varepsilon \mathcal{W}_{\text{und}} = -\frac{2\pi}{(y+\varepsilon)^2} \left[ cE\left(\frac{1}{c}\right) - \varepsilon \frac{c+1}{c} K\left(\frac{1}{c}\right) - \varepsilon \left(1 + \frac{y}{y+\varepsilon}\right) K\left(\frac{y}{y+\varepsilon}\right) \right]. \quad (6.13)$$

Putting (6.9), (6.12), and (6.13) into (6.8), it follows

$$\begin{aligned}\partial_c \mathcal{W}(\mathbb{T}_{D,c}) &= \partial_c \mathcal{W}_{\text{nod}} + \partial_\varepsilon \mathcal{W}_{\text{und}} + \partial_y \mathcal{W}_{\text{und}} \cdot y' \\ &= 2\pi E\left(\frac{1}{c}\right) - \frac{2\pi}{(y+\varepsilon)^2} \left[ cE\left(\frac{1}{c}\right) - \varepsilon \frac{c+1}{c} K\left(\frac{1}{c}\right) - \varepsilon \left(1 + \frac{y}{y+\varepsilon}\right) K\left(\frac{y}{y+\varepsilon}\right) \right] \\ &\quad + \frac{2\pi\varepsilon}{(y+\varepsilon)^2} \left[ E\left(\frac{1}{c}\right) - K\left(\frac{1}{c}\right) - K\left(\frac{y}{y+\varepsilon}\right) \right] - \frac{2\pi\varepsilon^2 y}{(y+\varepsilon)^3} z K\left(\frac{y}{y+\varepsilon}\right) \\ &= 2\pi E\left(\frac{1}{c}\right) \left[ 1 - \frac{c}{(y+\varepsilon)^2} + \frac{\varepsilon}{(y+\varepsilon)^2} \right] + \frac{2\pi\varepsilon}{(y+\varepsilon)^2} K\left(\frac{1}{c}\right) \left[ \frac{c+1}{c} - 1 \right] + \frac{2\pi\varepsilon y}{(y+\varepsilon)^3} K\left(\frac{y}{y+\varepsilon}\right) [1 - \varepsilon z] \\ &= 2\pi \left(1 - \frac{1}{(y+\varepsilon)^2}\right) E\left(\frac{1}{c}\right) + \frac{2\pi}{c(y+\varepsilon)^2} \varepsilon K\left(\frac{1}{c}\right) + \frac{2\pi y}{(y+\varepsilon)^3} (1 - \varepsilon z) \varepsilon K\left(\frac{y}{y+\varepsilon}\right).\end{aligned}$$

Therefore,

$$\frac{\partial_c \mathcal{W}(\mathbb{T}_{D,c})}{2\pi} = a_1 \left(1 - \frac{1}{(y+\varepsilon)^2}\right) + a_2 \varepsilon K\left(\frac{1}{c}\right) + a_3 \varepsilon K\left(\frac{y}{y+\varepsilon}\right) \quad (6.14)$$

with  $a_1, a_2, a_3$  depending on  $c$ . Recalling that

$$\varepsilon K\left(\frac{1}{c}\right) \xrightarrow{c \downarrow 1} 0, \quad \varepsilon K\left(\frac{y}{y+\varepsilon}\right) \xrightarrow{c \downarrow 1} 0, \quad \varepsilon y' \xrightarrow{c \downarrow 1} 0, \quad y' \xrightarrow{c \downarrow 1} -\infty, \quad y \xrightarrow{c \downarrow 1} 1 \quad (6.15)$$

we in particular see  $a_1, a_2, a_3 \rightarrow 1$  as  $c \rightarrow 1$  and hence  $\partial_c \mathcal{W}(\mathbb{T}_{D,c}) \rightarrow 0$  as  $c \rightarrow 1$ . We claim that

$$\lim_{c \rightarrow 1+} \frac{\varepsilon K\left(\frac{1}{c}\right) + \varepsilon K\left(\frac{y}{y+\varepsilon}\right)}{1 - \frac{1}{(y+\varepsilon)^2}} = -\frac{1}{2}. \quad (6.16)$$

In view of (6.15), it follows

$$\begin{aligned}\frac{\varepsilon}{1+y'} \partial_c K\left(\frac{1}{c}\right) &= \frac{\varepsilon}{1+y'} \left[ \frac{E(\frac{1}{c})}{1-\frac{1}{c^2}} - K\left(\frac{1}{c}\right) \right] c \frac{-1}{c^2} \xrightarrow{c \downarrow 1} 0, \\ \partial_c \frac{y}{y+\varepsilon} &= y' \partial_y \frac{y}{y+\varepsilon} + \partial_\varepsilon \frac{y}{y+\varepsilon} = \frac{\varepsilon y' - y}{(y+\varepsilon)^2} \xrightarrow{c \downarrow 1} -1, \\ \frac{\varepsilon}{1+y'} \partial_c K\left(\frac{y}{y+\varepsilon}\right) &= \frac{\varepsilon}{1+y'} \left[ \frac{E(\frac{y}{y+\varepsilon})}{1-\frac{y^2}{(y+\varepsilon)^2}} - K\left(\frac{y}{y+\varepsilon}\right) \right] \frac{y+\varepsilon}{y} \partial_c \frac{y}{y+\varepsilon} \xrightarrow{c \downarrow 1} 0.\end{aligned}$$

Thus, by L'Hôpital's rule and (6.7),

$$\lim_{c \rightarrow 1+} \frac{\varepsilon K(\frac{1}{c}) + \varepsilon K(\frac{y}{y+\varepsilon})}{1 - \frac{1}{(y+\varepsilon)^2}} = \lim_{c \rightarrow 1+} \frac{K(\frac{1}{c}) + K(\frac{y}{y+\varepsilon})}{\frac{2}{(y+\varepsilon)^3} [1 + y']} = -\frac{1}{2}$$

which proves (6.16). By (6.16) and (6.14), one infers

$$\partial_c \mathcal{W}(\mathbb{T}_{D,c}) < 0 \quad \text{for } c \text{ close to } 1.$$

Therefore, for some  $\gamma_0 > 1$ , there holds

$$\mathcal{W}(\mathbb{T}_{D,c}) < 8\pi \quad \text{whenever } 1 < c < \gamma_0. \quad (6.17)$$

By the Li–Yau inequality [LY82] we see that the Delaunay tori  $\mathbb{T}_{D,c}$  are embedded, the profile curve is a simple closed curve, the genus is 1, and the algebraic volume (1.2) is the enclosed volume (up to orientation). Combining (4.8), (4.9), (5.11), and (5.12), we infer

$$\lim_{c \rightarrow 1+} \text{iso}(\mathbb{T}_{D,c}) = \infty.$$

Together with (6.17), this proves Theorem 1.1. It remains to mention that, since the profile curve is  $C^{1,1}$ -regular as discussed at the beginning of this section, the resulting surfaces of revolution  $\mathbb{T}_{D,c}$  are also  $C^{1,1}$ -regular.  $\square$

**Proof of Corollary 1.3.** Let  $\mathbb{T}^2$  be an abstract 2-dimensional torus. Denote with  $\mathcal{E}_{\mathbb{S}^2}$  and  $\mathcal{E}_{\mathbb{T}^2}$  the spaces of Lipschitz immersions of  $\mathbb{S}^2$  and  $\mathbb{T}^2$  into  $\mathbb{R}^3$  as defined in Section 2.2 of [KMR14]. By SCHYGULLA [Sch12] and [KMR14, Theorem 1.1] the following holds true. For each  $\sigma > \sqrt[3]{36\pi}$ , there exists a smoothly embedded spherical surface  $\mathbb{S}_{S,\sigma}$  with

$$\mathcal{W}(\mathbb{S}_{S,\sigma}) = \beta_0(\sigma) := \inf\{\mathcal{W}(\vec{\Phi}) \mid \vec{\Phi} \in \mathcal{E}_{\mathbb{S}^2}, \text{iso}(\vec{\Phi}) = \sigma\}.$$

Moreover, by Theorem 1.6 in KELLER–MONDINO–RIVIÈRE [KMR14], for each  $\sigma_0$  in the set

$$I_1 := \left\{ \sigma \in \mathbb{R} \left| \inf_{\substack{\vec{\Phi} \in \mathcal{E}_{\mathbb{T}^2} \\ \text{iso}(\vec{\Phi}) = \sigma}} \mathcal{W}(\vec{\Phi}) < \min\{8\pi, 2\pi^2 + \beta_0(\sigma) - 4\pi\} \right. \right\} \subset (\sqrt[3]{36\pi}, \infty)$$

there exists a smoothly embedded torus  $\Sigma_0$  in  $\mathbb{R}^3$  with

$$\mathcal{W}(\Sigma_0) = \beta_1(\sigma_0) := \inf_{\substack{\vec{\Phi} \in \mathcal{E}_{\mathbb{T}^2} \\ \text{iso}(\vec{\Phi}) = \sigma_0}} \mathcal{W}(\vec{\Phi}).$$

From Corollary 1.5 in MONDINO–SCHARRER [MS21] it follows

$$I_1 = \{\sigma \in \mathbb{R} \mid \beta_1(\sigma) < 8\pi\}.$$

Recall that the function  $\beta_1(\cdot)$  is non-decreasing on the set  $I_1$ . This can be shown using Möbius transformations, see for instance [Sch21, Proposition 1] and [YC22, Theorem 3.1]. Therefore, the set  $I_1$  is in fact an interval. Moreover, each  $C^{1,1}$ -embedding of  $\mathbb{T}^2$  into  $\mathbb{R}^3$  is in particular a Lipschitz immersion, i.e. a member of the space  $\mathcal{E}_{\mathbb{T}^2}$ . Thus, by Theorem 1.1,

$$I_1 = (\sqrt[3]{36\pi}, \infty)$$

which proves Corollary 1.3.  $\square$

**Proof of Corollary 1.5.** Denote with  $\alpha_c : \mathbb{S}^2 \rightarrow \mathbb{R}^2$  the  $C^{1,1}$ -regular profile curve of the Delaunay tori  $\mathbb{T}_{D,c}$  corresponding to  $1 < c < \gamma_0$ . In view of (4.6) and (5.5), we have indeed that  $\alpha_c$  takes values in the half space  $\mathbb{H}^2 := \{(x, y) \in \mathbb{R}^2 \mid x > 0\}$ . Let  $\alpha_c^\varepsilon$  be the mollification of  $\alpha_c$  for  $\varepsilon > 0$  and let  $T_{\alpha_c^\varepsilon}$  be the corresponding rotationally symmetric torus. Then,

$$T_{\alpha_c^\varepsilon} \rightarrow \mathbb{T}_{D,c} \quad \text{as } \varepsilon \downarrow 0 \text{ in } W^{2,p} \text{ for all } p > 1.$$

In particular, for  $\varepsilon > 0$  small, we have that  $\alpha_c^\varepsilon \in C^\infty(\mathbb{S}^1, \mathbb{H}^2)$  and, by Theorem 1.1,  $\mathcal{W}(T_{\alpha_c^\varepsilon}) < 8\pi$ . Following [DMSS20, Equation (2.6)], we define

$$\mathcal{L}_{\mathbb{H}^2}(\gamma) := \int_0^1 \frac{|\gamma'|}{\gamma^1} dx \quad \text{for all } \gamma = (\gamma^1, \gamma^2) \in C^1(\mathbb{S}^1, \mathbb{H}^2).$$

Using (4.2) and (4.4), we see

$$\int_0^{2\pi} \frac{|(f, g)'|}{f} dt = a \int_0^{2\pi} \frac{dt}{\sqrt{a^2 - c^2 \cos^2(t)}} \xrightarrow{b \downarrow 0} \int_0^{2\pi} \frac{dt}{|\sin(t)|} = \infty. \quad (6.18)$$

Similarly, using (5.1), (5.3), and  $\int \frac{1}{\sinh(t)} = \log |\tanh(t/2)| + C$ ,

$$\int_{-\infty}^{\infty} \frac{|(f_\pm, f_\pm)'|}{f_\pm} dt = a \int_{-\infty}^{\infty} \frac{dt}{\sqrt{c^2 \cosh^2(t) - a^2}} \xrightarrow{b \downarrow 0} \int_{-\infty}^{\infty} \frac{dt}{|\sinh(t)|} = \infty. \quad (6.19)$$

Hence, combining (6.18) and (6.19), it follows that

$$\mathcal{L}_{\mathbb{H}^2}(\alpha_c) \rightarrow \infty \quad \text{as } c \downarrow 1.$$

Moreover, for all  $1 < c < \gamma_0$ , there holds

$$\mathcal{L}_{\mathbb{H}^2}(\alpha_c^\varepsilon) \rightarrow \mathcal{L}_{\mathbb{H}^2}(\alpha_c) \quad \text{as } \varepsilon \downarrow 0.$$

Finally, since by [DMSS20, Proposition 4.2.], the conformal class  $\omega(T_\gamma)$  of any rotationally symmetric torus  $T_\gamma$  corresponding to a profile curve  $\gamma \in C^\infty(\mathbb{S}^1, \mathbb{H}^2)$  is given by

$$\omega(T_\gamma) = \begin{cases} i \frac{1}{2\pi} \mathcal{L}_{\mathbb{H}^2}(\gamma) & \mathcal{L}_{\mathbb{H}^2}(\gamma) \geq 2\pi \\ i \frac{2\pi}{\mathcal{L}_{\mathbb{H}^2}(\gamma)} & \mathcal{L}_{\mathbb{H}^2}(\gamma) < 2\pi \end{cases},$$

the conclusion follows.  $\square$

## 7 Delaunay spheres of high isoperimetric ratio

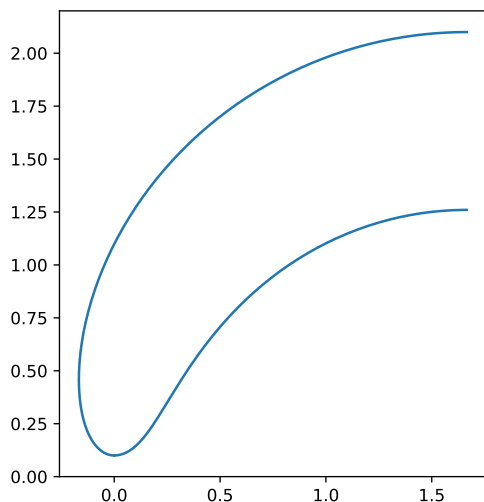


Figure 7: Profile curve of half a Delaunay torus with  $c = 1.1$

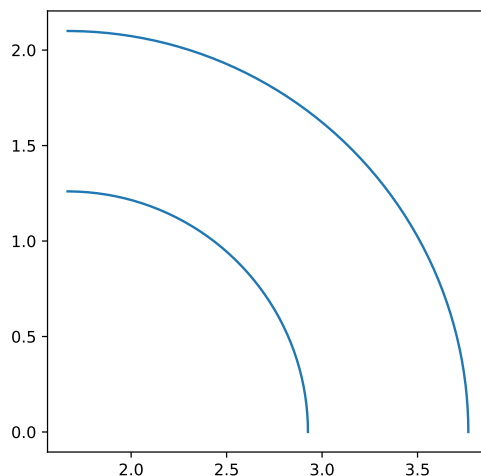


Figure 8: Concentric quarter circles fitting into half a Delaunay torus.

The Delaunay tori  $\mathbb{T}_{D,c}$  corresponding to  $1 < c < \gamma_0$  can be used to construct spheres with analogous properties. The first part of the construction works just like the construction of the Delaunay tori only that now, both the nodoid and the unduloid run only for half a period instead of one full period. To be more precise, both the nodoid and the unduloid now only run from the point where  $f_+$ ,  $f$  attain their minimum according to (4.6), (5.5) up to the point where  $f_-$ ,  $f$  reach their maximum (according to (4.6), (5.5)) but not until  $f_+$ ,  $f$  reach their minimum again. This results in half a Delaunay torus, see Figure 7. Notice that unduloids and nodoids are symmetric around their maxima ( $t = \pi$  in (4.2), (4.3) for unduloids;  $t = 0$  in (5.1), (5.2) for nodoids). Thus, the Willmore energy of this particular half of a Delaunay torus is indeed half the Willmore energy of a whole Delaunay torus. Let  $c, y, a$  be the balancing parameters according to (6.1) and (6.2). Then the maxima of the nodoid and the unduloid are given by  $c + 1$  and  $a + y$ , respectively. Next, take two concentric circular sectors with radii  $c + 1$  and  $a + y$  both of which being one quarter of a full circle, see Figure 8. Choose the centre of the two circular

sectors at  $L/2$  on the axis of rotation of the half Delaunay torus, where  $L = 4aE(y/a)$  (see (4.7)). Then, the two circular sectors fit right into the half Delaunay torus, resulting in a  $C^{1,1}$ -curve. Since the two circular sectors meet the axis of rotation perpendicular, the resulting surface of revolution is  $C^{1,1}$ -regular too. It is of sphere type. The full profile can be seen in Figure 9. The resulting family of surfaces is called *Delaunay spheres*. Since  $a + y, c + 1 \xrightarrow{c \downarrow 1} 2$ , the Delaunay spheres converge as varifolds to a sphere of multiplicity 2 as  $c \rightarrow 1$ . Their Willmore energy is given by

$$\mathcal{W}(\mathbb{S}_{D,c}) = 4\pi + \frac{\mathcal{W}(\mathbb{T}_{D,c})}{2}.$$

Similarly as in the proof of Theorem 1.1, we can combine (4.8), (4.9), (5.11), and (5.12) to see  $\text{iso}(\mathbb{S}_{D,c}) \rightarrow \infty$  as  $c \rightarrow 1$  which concludes the proof of Theorem 1.2.  $\square$

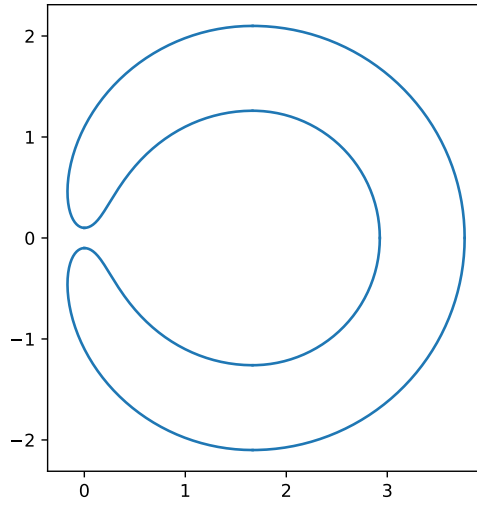


Figure 9: Profile of a Delaunay sphere with  $c = 1.1$

## 8 Helfrich tori with small spontaneous curvature

Suppose  $A_0, V_0 > 0$  satisfy the isoperimetric inequality:  $A_0^3 > 36\pi V_0^2$  and let

$$\mathcal{S}_1(A_0, V_0) = \{f \in \mathcal{S}_1 \mid \text{area}(f) = A_0, \text{vol}(f) = V_0\}.$$

Notice that if  $c_0 = 0$ , then the Helfrich functional reduces to the Willmore functional:  $\mathcal{H}_0 = \mathcal{W}$ . Moreover, one can show (see [MS20, Equation 4.26])

$$\left| \inf_{f \in \mathcal{S}_1(A_0, V_0)} \sqrt{\mathcal{W}(f)} - \inf_{f \in \mathcal{S}_1(A_0, V_0)} \sqrt{\mathcal{H}_{c_0}(f)} \right| \leq |c_0| \sqrt{A_0}. \quad (8.1)$$

In particular, the minimal Helfrich energy is continuous with respect to  $c_0$  at  $c_0 = 0$ . For the case  $c_0 = 0$ , existence of smoothly embedded minimisers with given fixed area and

volume corresponds to Corollary 1.3 in [KMR14]. Corollary 1.4 states that minimisers remain embedded for  $c_0$  close to zero. Moreover, (by the choice of  $\varepsilon(A_0, V_0)$  in (1.4)) a minimising sequence for  $c_0 = 0$  has the same uniform bounds on the Willmore energy as a minimising sequence for  $c_0$  close to zero. Indeed, we will see that the compactness proof in [KMR14] still works for  $c_0$  close to zero. However, for general  $c_0$ , minimisers are no longer embedded, see [MS20]. The following proof is a combination of four independent results: the two strict inequalities Theorem 1.1 and [MS21, Corollary 1.5] are needed to deduce that  $\varepsilon(A_0, V_0)$  (as defined in (1.4)) is strictly positive; then, one can apply the compactness proof of [KMR14]; finally, one can conclude the regularity from [MS20] (after RIVIÈRE [Riv08]).

In order to prove Corollary 1.4, let  $\vec{\Phi}_k$  be a minimising sequence of

$$\inf\{\mathcal{H}_{c_0}(\vec{\Phi}) \mid \vec{\Phi} \in \mathcal{E}_{\mathbb{T}^2}, \text{area}(\vec{\Phi}) = A_0, \text{vol}(\vec{\Phi}) = V_0\}.$$

Recall the definition of  $\varepsilon(A_0, V_0)$  in Equation (1.4):

$$\varepsilon(A_0, V_0) := \frac{\sqrt{\min\{8\pi, 2\pi^2 + \beta_0(A_0/V_0^{2/3}) - 4\pi\}} - \sqrt{\beta_1(A_0/V_0^{2/3})}}{2\sqrt{A_0}}.$$

By Theorem 1.1 and [MS21, Corollary 1.5], there holds  $\varepsilon(A_0, V_0) > 0$ . Using the continuity property (8.1) one can show for  $|c_0| < \varepsilon(A_0, V_0)$  that (see the proof of Lemma 4.4 in [MS20])

$$\limsup_{k \rightarrow \infty} \sqrt{\mathcal{W}(\vec{\Phi}_k)} < \sqrt{\beta_1(A_0/V_0^{2/3})} + 2\varepsilon(A_0, V_0)\sqrt{A_0}.$$

Thus, by the definition of  $\varepsilon(A_0, V_0)$  it follows

$$\limsup_{k \rightarrow \infty} \mathcal{W}(\vec{\Phi}_k) < 8\pi \tag{8.2}$$

and

$$\limsup_{k \rightarrow \infty} \mathcal{W}(\vec{\Phi}_k) < 2\pi^2 + \beta_0(A_0/V_0^{2/3}) - 4\pi. \tag{8.3}$$

In Section 4.3 of [KMR14] it is shown that due to the strict inequality in (8.3), the conformal factors of  $\vec{\Phi}_k$  are bounded away from finitely many concentration points  $a_1, \dots, a_N$  in  $\mathbb{T}^2$ . Hence, by the uniform energy bound in (8.2), there exists  $\vec{\Phi}_\infty \in \mathcal{E}_{\mathbb{T}^2}$  such that (after passing to a subsequence and after re-parametrising) for all  $\delta > 0$

$$\vec{\Phi}_k \rightarrow \vec{\Phi}_\infty \quad \text{as } k \rightarrow \infty \text{ weakly in } W^{2,2}(\mathbb{T}^2 \setminus \bigcup_{i=1}^N B_\delta(a_i), \mathbb{R}^3). \tag{8.4}$$

Moreover, in Section 4.2 of [KMR14] it is shown that due to (8.2), there hold that

$$\lim_{k \rightarrow \infty} \text{vol}(\vec{\Phi}_k) = \text{vol}(\vec{\Phi}_\infty), \quad \lim_{k \rightarrow \infty} \text{area}(\vec{\Phi}_k) = \text{area}(\vec{\Phi}_\infty).$$

After the mentioned re-parametrisations, the  $\vec{\Phi}_k$ 's are weakly conformal which implies  $\Delta_k \vec{\Phi}_k = 2H_{\vec{\Phi}_k}$  where in any local chart  $x$ , the intrinsic Laplacians  $\Delta_k$  are given by

$$\Delta_k \vec{\Phi} = \frac{1}{\sqrt{g_k}} \partial_{x^i} (\sqrt{g_k} (g_k)^{ij} \partial_{x^j} \vec{\Phi}), \quad g_k = \det(g_k)_{ij}$$



for all  $\vec{\Phi} \in W^{2,2}(\mathbb{T}^2, \mathbb{R}^3)$  where  $(g_k)_{ij} = \partial_{x^i} \vec{\Phi}_k \cdot \partial_{x^j} \vec{\Phi}_k$  and  $(g_k)^{ij}$  is the inverse of  $(g_k)_{ij}$ . Therefore, by the weak convergence (8.4) it follows that for all  $\delta > 0$ ,

$$\lim_{k \rightarrow \infty} \int_{\mathbb{T}^2 \setminus \bigcup_{i=1}^N B_\delta(a_i)} H_{\vec{\Phi}_k} d\mu_{\vec{\Phi}_k} = \int_{\mathbb{T}^2 \setminus \bigcup_{i=1}^N B_\delta(a_i)} H_{\vec{\Phi}_\infty} d\mu_{\vec{\Phi}_\infty}.$$

Moreover, by [KMR14, Equation (4.7)],

$$\liminf_{\delta \rightarrow 0} \liminf_{k \rightarrow \infty} \int_{B_\delta(a_i)} 1 d\mu_{\vec{\Phi}_k} = 0$$

for all  $i \in \{1, \dots, N\}$ . Using the Cauchy–Schwarz inequality and the uniform bound on the Willmore energy (8.2), it follows that after passing to a subsequence

$$\lim_{k \rightarrow \infty} \int_{\mathbb{T}^2} H_{\vec{\Phi}_k} d\mu_{\vec{\Phi}_k} = \int_{\mathbb{T}^2} H_{\vec{\Phi}_\infty} d\mu_{\vec{\Phi}_\infty}.$$

Thus, by lower semi continuity of the Willmore functional under the convergence of (8.4),

$$\mathcal{H}_{c_0}(\vec{\Phi}_\infty) \leq \liminf_{k \rightarrow \infty} \mathcal{H}_{c_0}(\vec{\Phi}_k), \quad \mathcal{W}(\vec{\Phi}_\infty) < 8\pi.$$

Therefore,  $\vec{\Phi}_\infty$  is a minimiser and, by the Li–Yau inequality,  $\vec{\Phi}_\infty \in W^{2,2}(\mathbb{T}^2, \mathbb{R}^3)$  is an embedding without branch points since branch points have multiplicity at least 2 according to [KL12, Theorem 3.1]. Moreover, by the regularity result [MS20, Theorem 4.3] (after [Riv08]),  $\vec{\Phi}_\infty \in C^\infty(\mathbb{T}^2, \mathbb{R}^3)$  which completes the proof of Corollary 1.4.  $\square$

## References

- [BBM14] Enrique Bendito, Mark J. Bowick, and Agustín Medina. A natural parameterization of the roulettes of the conics generating the Delaunay surfaces. *J. Geom. Symmetry Phys.*, 33:27–45, 2014.
- [BdC84] João Lucas Barbosa and Manfredo do Carmo. Stability of hypersurfaces with constant mean curvature. *Math. Z.*, 185(3):339–353, 1984.
- [BF71] Paul F. Byrd and Morris D. Friedman. *Handbook of elliptic integrals for engineers and scientists*. Die Grundlehren der mathematischen Wissenschaften, Band 67. Springer-Verlag, New York-Heidelberg, 1971. Second edition, revised.
- [Bla09] Simon Blatt. A singular example for the Willmore flow. *Analysis (Munich)*, 29(4):407–430, 2009.
- [BLS20] Katharina Brazda, Luca Lussardi, and Ulisse Stefanelli. Existence of varifold minimizers for the multiphase Canham-Helfrich functional. *Calc. Var. Partial Differential Equations*, 59(3):Paper No. 93, 26, 2020.

- [CV13] Rustum Choksi and Marco Veneroni. Global minimizers for the doubly-constrained Helfrich energy: the axisymmetric case. *Calc. Var. Partial Differential Equations*, 48(3-4):337–366, 2013.
- [CVG07] Pavel Castro-Villarreal and Jemal Guven. Inverted catenoid as a fluid membrane with two points pulled together. *Physical Review E*, 76(1):011922, 2007.
- [Del41] Charles E. Delaunay. Sur la surface de révolution dont la courbure moyenne est constante. *J. Math. Pures Appl.*, 6:309–314, 1841.
- [DMSS20] Anna Dall’Acqua, Marius Müller, Reiner Schätzle, and Adrian Spener. The willmore flow of tori of revolution, 2020.
- [Eic20] Sascha Eichmann. Lower semicontinuity for the Helfrich problem. *Ann. Global Anal. Geom.*, 58(2):147–175, 2020.
- [Hel73] Wolfgang Helfrich. Elastic properties of lipid bilayers: theory and possible experiments. *Zeitschrift für Naturforschung C*, 28(11-12):693–703, 1973.
- [Hél02] Frédéric Hélein. *Harmonic maps, conservation laws and moving frames*, volume 150 of *Cambridge Tracts in Mathematics*. Cambridge University Press, Cambridge, second edition, 2002. Translated from the 1996 French original, With a foreword by James Eells.
- [HMO07] Mariana Hadzhilazova, Ivailo M. Mladenov, and John Oprea. Unduloids and their geometry. *Arch. Math. (Brno)*, 43(5):417–429, 2007.
- [HN21] Lynn Heller and Cheikh Birahim Ndiaye. First explicit constrained Willmore minimizers of non-rectangular conformal class. *Adv. Math.*, 386:Paper No. 107804, 47, 2021.
- [IT92] Y. Iwayoshi and M. Taniguchi. *An introduction to Teichmüller spaces*. Springer-Verlag, Tokyo, 1992. Translated and revised from the Japanese by the authors.
- [Kap91] Nicolaos Kapouleas. Compact constant mean curvature surfaces in Euclidean three-space. *J. Differential Geom.*, 33(3):683–715, 1991.
- [Kap95] Nikolaos Kapouleas. Constant mean curvature surfaces constructed by fusing Wente tori. *Invent. Math.*, 119(3):443–518, 1995.
- [KKS89] Nicholas J. Korevaar, Rob Kusner, and Bruce Solomon. The structure of complete embedded surfaces with constant mean curvature. *J. Differential Geom.*, 30(2):465–503, 1989.
- [KL12] Ernst Kuwert and Yuxiang Li.  $W^{2,2}$ -conformal immersions of a closed Riemann surface into  $\mathbb{R}^n$ . *Comm. Anal. Geom.*, 20(2):313–340, 2012.

- [KL18] Ernst Kuwert and Yuxiang Li. Asymptotics of Willmore minimizers with prescribed small isoperimetric ratio. *SIAM J. Math. Anal.*, 50(4):4407–4425, 2018.
- [KMR14] Laura G. A. Keller, Andrea Mondino, and Tristan Rivière. Embedded surfaces of arbitrary genus minimizing the Willmore energy under isoperimetric constraint. *Arch. Ration. Mech. Anal.*, 212(2):645–682, 2014.
- [KP86] Wolfgang Kühnel and Ulrich Pinkall. On total mean curvatures. *Quart. J. Math. Oxford Ser. (2)*, 37(148):437–447, 1986.
- [KS04] Ernst Kuwert and Reiner Schätzle. Removability of point singularities of Willmore surfaces. *Ann. of Math. (2)*, 160(1):315–357, 2004.
- [KS13] Ernst Kuwert and Reiner Schätzle. Minimizers of the Willmore functional under fixed conformal class. *J. Differential Geom.*, 93(3):471–530, 2013.
- [Kus89] Rob Kusner. Comparison surfaces for the Willmore problem. *Pacific J. Math.*, 138(2):317–345, 1989.
- [Law70] H. Blaine Lawson, Jr. Complete minimal surfaces in  $S^3$ . *Ann. of Math. (2)*, 92:335–374, 1970.
- [LY82] Peter Li and Shing Tung Yau. A new conformal invariant and its applications to the Willmore conjecture and the first eigenvalue of compact surfaces. *Invent. Math.*, 69(2):269–291, 1982.
- [MO03] Ivaïlo Mladenov and John Oprea. Unduloids and their closed-geodesics. In *Geometry, integrability and quantization (Sts. Constantine and Elena, 2002)*, pages 206–234. Coral Press Sci. Publ., Sofia, 2003.
- [MP01] Rafe Mazzeo and Frank Pacard. Constant mean curvature surfaces with Delaunay ends. *Comm. Anal. Geom.*, 9(1):169–237, 2001.
- [MR14] Stefan Müller and Matthias Röger. Confined structures of least bending energy. *J. Differential Geom.*, 97(1):109–139, 2014.
- [MŠ95] Stefan Müller and Vladimír Šverák. On surfaces of finite total curvature. *J. Differential Geom.*, 42(2):229–258, 1995.
- [MS20] Andrea Mondino and Christian Scharrer. Existence and regularity of spheres minimising the Canham-Helfrich energy. *Arch. Ration. Mech. Anal.*, 236(3):1455–1485, 2020.
- [MS21] Andrea Mondino and Christian Scharrer. A strict inequality for the minimization of the Willmore functional under isoperimetric constraint. *Advances in Calculus of Variations*, 2021.

- [NS14] Cheikh Birahim Ndiaye and Reiner Michael Schätzle. Explicit conformally constrained Willmore minimizers in arbitrary codimension. *Calc. Var. Partial Differential Equations*, 51(1-2):291–314, 2014.
- [NS15] Cheikh Birahim Ndiaye and Reiner Michael Schätzle. New examples of conformally constrained Willmore minimizers of explicit type. *Adv. Calc. Var.*, 8(4):291–319, 2015.
- [Riv08] Tristan Rivière. Analysis aspects of Willmore surfaces. *Invent. Math.*, 174(1):1–45, 2008.
- [Riv13] Tristan Rivière. Lipschitz conformal immersions from degenerating Riemann surfaces with  $L^2$ -bounded second fundamental forms. *Adv. Calc. Var.*, 6(1):1–31, 2013.
- [Riv14] Tristan Rivière. Variational principles for immersed surfaces with  $L^2$ -bounded second fundamental form. *J. Reine Angew. Math.*, 695:41–98, 2014.
- [Riv15] Tristan Rivière. Critical weak immersed surfaces within sub-manifolds of the Teichmüller space. *Adv. Math.*, 283:232–274, 2015.
- [Sch12] Johannes Schygulla. Willmore minimizers with prescribed isoperimetric ratio. *Arch. Ration. Mech. Anal.*, 203(3):901–941, 2012.
- [Sch21] Christian Scharrer. On the minimisation of bending energies related to the willmore functional under constraints on area and volume, 2021. PhD thesis, *Institutional Repository of the University of Warwick*, 2021.
- [Sim93] Leon Simon. Existence of surfaces minimizing the Willmore functional. *Comm. Anal. Geom.*, 1(2):281–326, 1993.
- [Wil65] Thomas J. Willmore. Note on embedded surfaces. *An. Şti. Univ. “Al. I. Cuza” Iaşi Sect. I a Mat. (N.S.)*, 11B:493–496, 1965.
- [Woj17] Stephan Wojtowytsch. Helfrich’s energy and constrained minimisation. *Commun. Math. Sci.*, 15(8):2373–2386, 2017.
- [YC22] Thomas Yu and Jingmin Chen. Uniqueness of Clifford torus with prescribed isoperimetric ratio. *Proc. Amer. Math. Soc.*, 150(4):1749–1765, 2022.